Supporting Information

Yang *et al*. 10.1073/pnas.0802978105

SI Text

Note 1. Of the five glutamate transporters in the rain, three of them, EAAT1-EAAT3, are expressed in the hippocampus (1). EAAT1 and EAAT2 are glial transporters while EAAT3 are neuronal transporters. DL-TBOA inhibits all EAATs, whereas TFB-TBOA have much higher preference for EAAT1 and EAAT2 than for EAAT3 (IC_{50} are 17, 22, and 300 nM for EAAT1, EAAT2, and EAAT3 respectively). At 100 nM, TFB-TBOA should selectively inhibit EAAT1 and EAAT2 with only modest effects on EAAT3. DHK, on the other hand, selectively inhibits EAAT2 (IC_{50} are 23 μM for EAAT2 and over 3 mM for EAAT1 and EAAT3, respectively).

Note 2. Slice preparation and recordings These procedures have been published (2, 6). Briefly, coronal hippocampal sections (350 μm) were taken from postnatal day 13 (P13)-P18 rat pups (Sprague-Dawley) using a Leica VT1000 tissue slicer in 4°C artificial cerebral spinal fluid (ACSF) containing (in mM): 110 choline chloride, 25 $NaHCO_3$, 25 D-glucose, 7 $MgSO_4$, 2.5 KCl, 1.25 NaH_2PO_4, 11.6 Na ascorbate, 3.1 Na pyruvate and 0.5 $CaCl_2$. The recording ACSF contained (in mM): 127 NaCl, 2.5 KCl, 1.25 NaH_2PO_4, 25 $NaHCO_3$, 25 D-glucose, 2 $CaCl_2$ and 1 $MgCl_2$. Slices were allowed to recover for 30 min at 32°C. They were then transferred to a holding chamber at room temperature in ACSF containing (in mM): 127 NaCl, 2.5 KCl, 1.25 NaH_2PO_4, 25 $NaHCO_3$, 25 D-glucose, 2 $CaCl_2$ and 1 $MgCl_2$. Recording and imaging started at least 1 hr after recovery.

Slices were placed in a custom-made recording chamber on the stage of an Olympus BX61 W microscope (Olympus, Tokyo, Japan) and perfused at a rate of 1–2 ml/min with ACSF. All recording and imaging experiments were performed at 30–32°C. Whole-cell patch clamp recordings were made from pyramidal neurons in CA1 of hippocampus under visual guidance. CA1 pyramidal cells in the hippocampus were held in current clamp mode or voltage clamp mode throughout the experiments. EPSPs or EPSCs were recorded with Axopatch 700B amplifier and analyzed with pClamp 9.0 software (Molecular Devices). The initial slope of EPSPs or the peak amplitude of EPSCs was used to measure synaptic responses. For current–clamp recording, the recording pipette solution contained (in mM): 128 K-gluconate, 10 NaCl, 2 $MgCl_2$, 10 Hepes, 0.5 EGTA, 4 Na_2ATP, 0.4 NaGTP, 15 phosphocreatine, and 1 calcein, pH 7.3. Calcein is a biologically inert fluorescent dye that we used for labeling of the dendritic spines. For voltage clamp experiments, the recording solution contained (in mM): 130 CsMeSO3, 8 NaCl, 10 Hepes,1 GTP (Na^+ salt), 4 ATP (Mg^{2+} salt), 0.2 EGTA, pH 7.3. All experiments were carried out in the presence of a $GABA_A$ antagonist, picrotoxin (50 μM).

For the electrophysiology experiments without imaging, glass pipettes (tip diameter, 4–6 μm) filled with ACSF were placed in the S. radiatum to stimulate the presynaptic inputs. For combined recording and imaging experiments, synaptic inputs were stimulated using a glass pipette with 3 μm opening positioned at about 20–30 μm away from the imaged spines. Stimulation at 0.05 Hz was used to establish baseline synaptic responses. LTP was induced using theta-burst pairing protocol for current clamp experiments. Briefly, for current clamp experiments, the stimulation strength was set to evoke EPSPs between 5 and 8 mV. LTP was induced using theta-burst stimulation (TBS) protocol. A train of TBS consisted of five bursts of stimuli at 5 Hz and each burst contained five pulses at 100 Hz. Each train was repeated twice with a 20-s interval. During TBS, the postsynaptic cells were depolarized through current injection to ensure that at least three spikes were generated during each burst. For voltage–clamp experiments, LTP was induced by stimulating the presynaptic inputs at 1 Hz for 2 min while holding the postsynaptic cells at 0 mV. Low frequency stimulation (LFS) consisted of 1 Hz stimulation for 5 min. High frequency stimulation (HFS) consisted of 100 Hz for 300 ms.

Note 3. Image acquisition and analysis images were taken every 15 min at a resolution of 512 × 512 pixels per frame, and an average of two was used in some experiments. For each time point, a stack of images covering the entire 3D range of the spines were taken with a z-step size about 0.5 μm. 2D projections of 3D image stacks containing dendritic spines of interest were used for display. Image analysis was performed blind with the person analyzing the images having no knowledge of the identity of the samples during the analysis. Spines were distinguished from filopodia based our previous criteria (6). Analysis was performed on all spines in the image field that were well resolved, i.e., protruding tangentially from the dendrite and clearly separated from other spines. The volumes of spine heads were used as measurements of the size. Images were first thresholded to eliminate background fluorescence. The integrated fluorescence intensity inside a spine head was measured for individual spines at different time points and normalized to the fluorescence intensity of the dendrites from the same image stack to correct for potential changes in excitation (7). This fluorescence intensity is expected to be proportional to the accessible spine volume (7). Fold change (volume) was determined by averaged values after TBP over the averaged values before TBP.

1. Tzingounis AV, Wadiche JI (2007) Glutamate transporters: Confining runaway excitation by shaping synaptic transmission. *Nat Rev Neurosci* 8:935–947.
2. Yang Y, Wang XB, Frerking M. Zhou Q (2008) Spine expression and stabilization associated with long-term potentiation. *J Neurosci* 28:5740–5751.
3. Edwards FA (1995) Anatomy and electrophysiology of fast central synapses lead to a structural model of long-term potentiation. *Physiol Rev* 75:759–787.
4. Lûscher C, Nicoll RA, Malenka RC, Muller D (2000) Synaptic plasticity and dynamic modulation of the postsynaptic membrane. *Nat Neurosci* 3:545–550.
5. Lisman J, Raghavachari S (2006) A unified model of the presynaptic and postsynaptic changes during LTP at CA1 synapses. *Sci STKE* 356:re 11.
6. Zhou Q, Homma KJ, Poo MM (2004) Shrinkage of dendritic spines associated with long-term depression of hippocampal synapses. *Neuron* 44:749–757.
7. Holtmaat AJ, *et al.* (2005) Transient and persistent dendritic spines in the neocortex in vivo. *Neuron* 45:279–291.

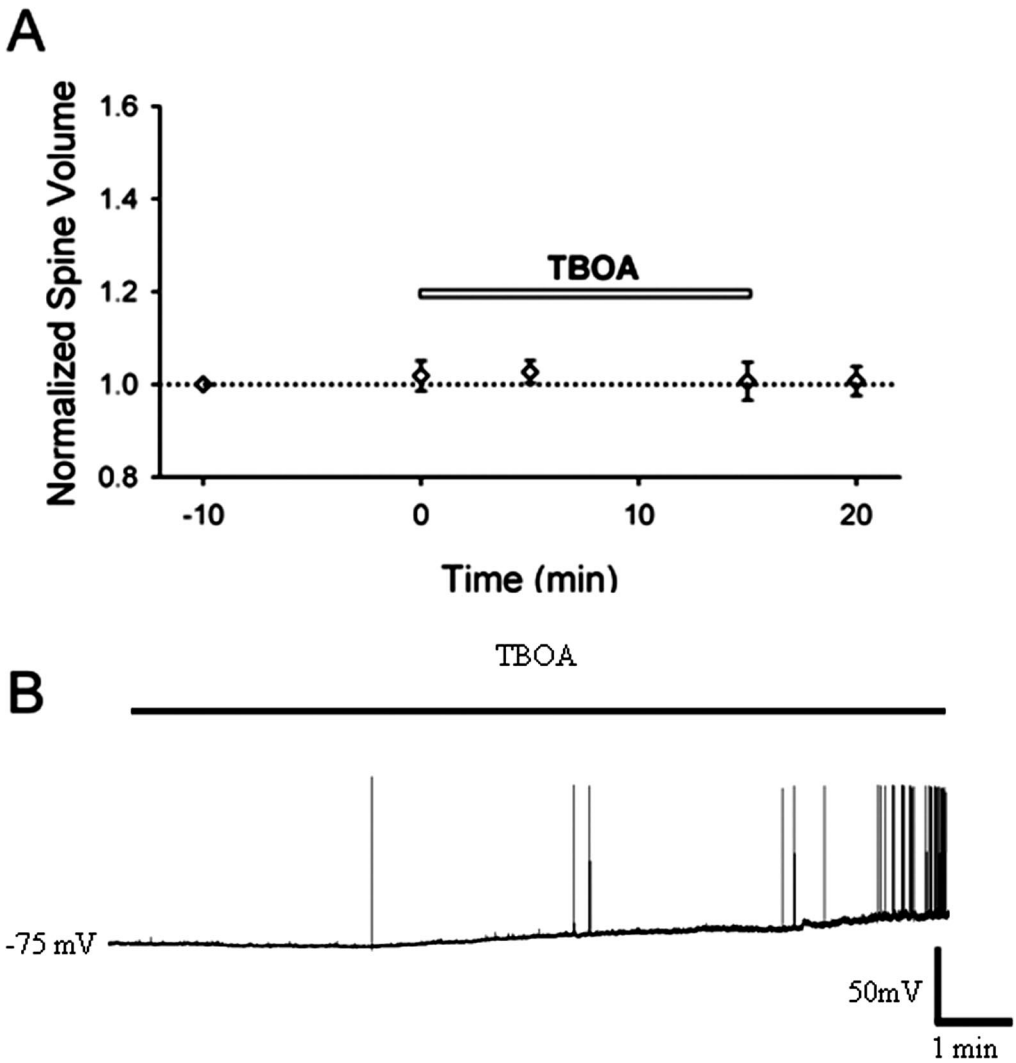

Fig. S1. Bath application of TBOA does not affect spine size or neuronal activity. (*A*) After establishing the spine volume under control conditions, TBOA was perfused for 15 min (bar) and had no effect on spine size ($n = 38$ spines/3 cells). (*B*) Bath application of TBOA did not affect neuronal activity within 5 min but did over 10 min.

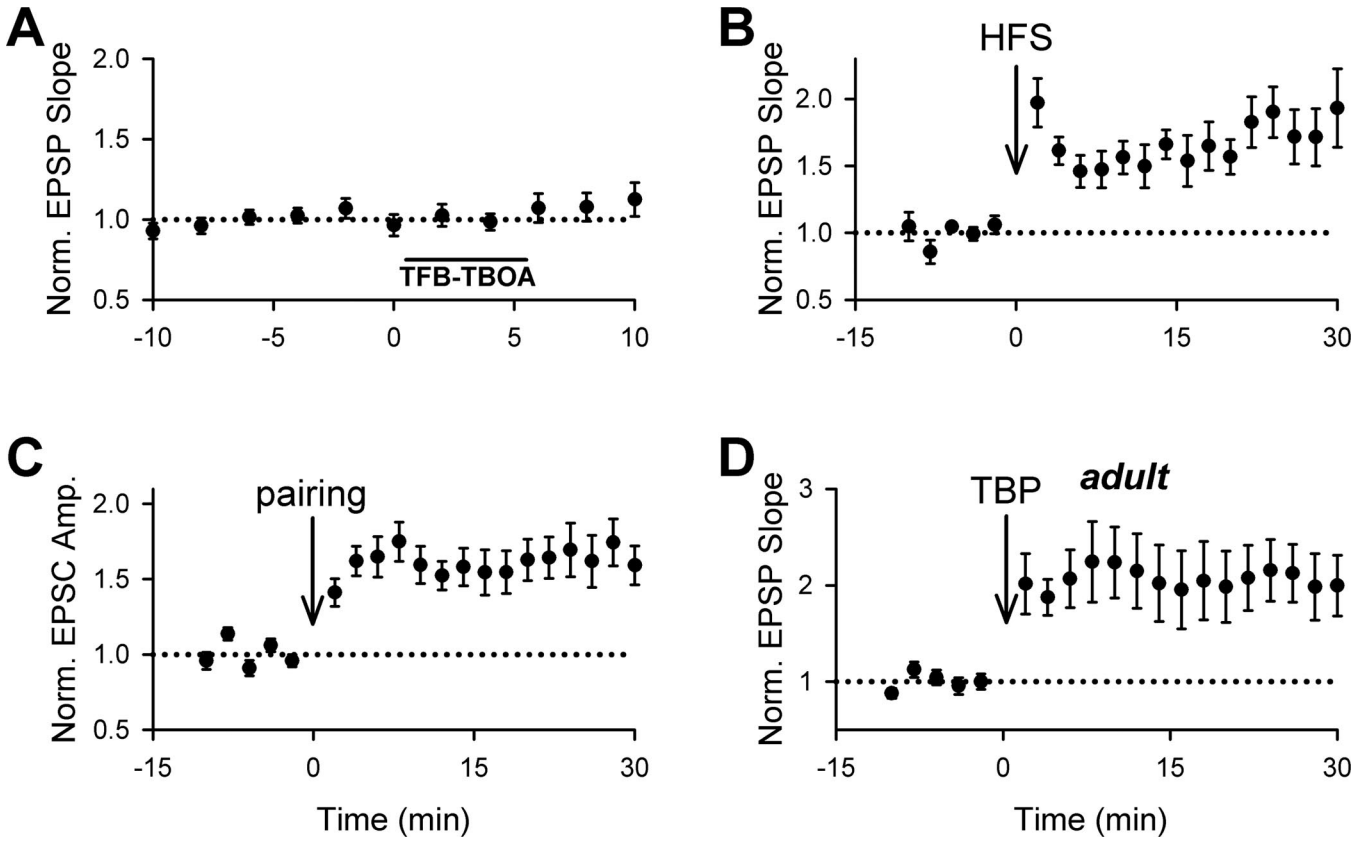

Fig. S2. LTP induced by different induction protocols. (*A*) Bath application of TFB-TBOA (bar) did not affect responses at naïve synapses. (*B*) Synaptic enhancement was readily observed after HFS (193 ± 29% at 30 min after induction, $n = 6$). (*C*) Voltage pairing induced an immediate increase in EPSC amplitude (175 ± 13% at 8 min after induction, $n = 12$). Pairing of presynaptic stimulation (2 min at 1 Hz) with the postsynaptic cells held at 0 mV was used for inducing LTP. (*D*) Large and stable potentiation in EPSPs was seen after TBP in adult hippocampal neurons (200 ± 32% at 30 min after induction, $n = 8$).

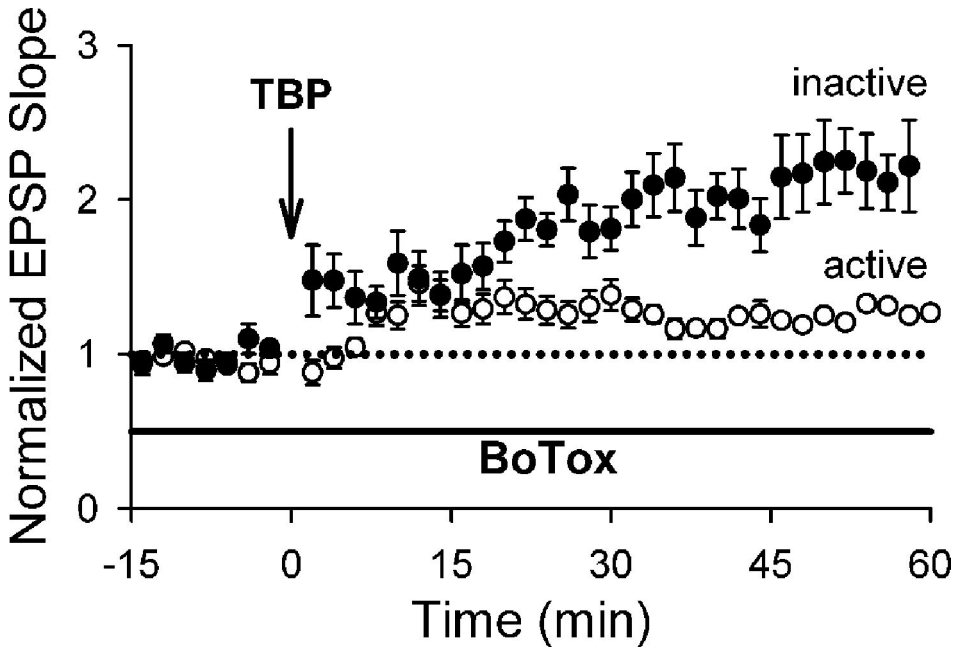

Fig. S3. Postsynaptic inhibition of exocytosis significantly reduces LTP. LTP was greatly inhibited in neurons loaded with BoTox via the recording patch pipette (123 ± 5% at 40 min after TBP; $n = 8$; $P < 0.01$, as compared with control LTP in Fig. 1*A*). Neurons loaded with heat-inactivated BoTox expressed normal LTP (200 ± 15% at 40 min after TBP; $n = 8$; $P = 0.85$, as compared to control LTP in Fig. 1*A*).

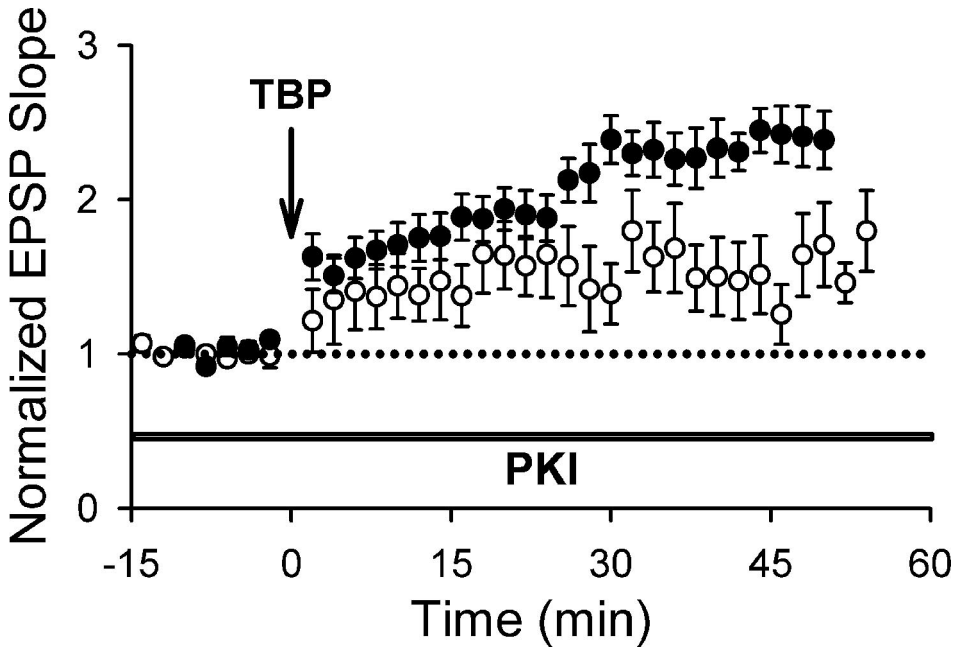

Fig. S4. Postsynaptic PKA activity is required for the full expression of LTP. Postsynaptic loading of PKI led to a significant reduction in LTP (153 ± 25% at 45–50 min after TBP, $n = 8$, open circles; $P < 0.05$, as compared with control LTP, filled circles).

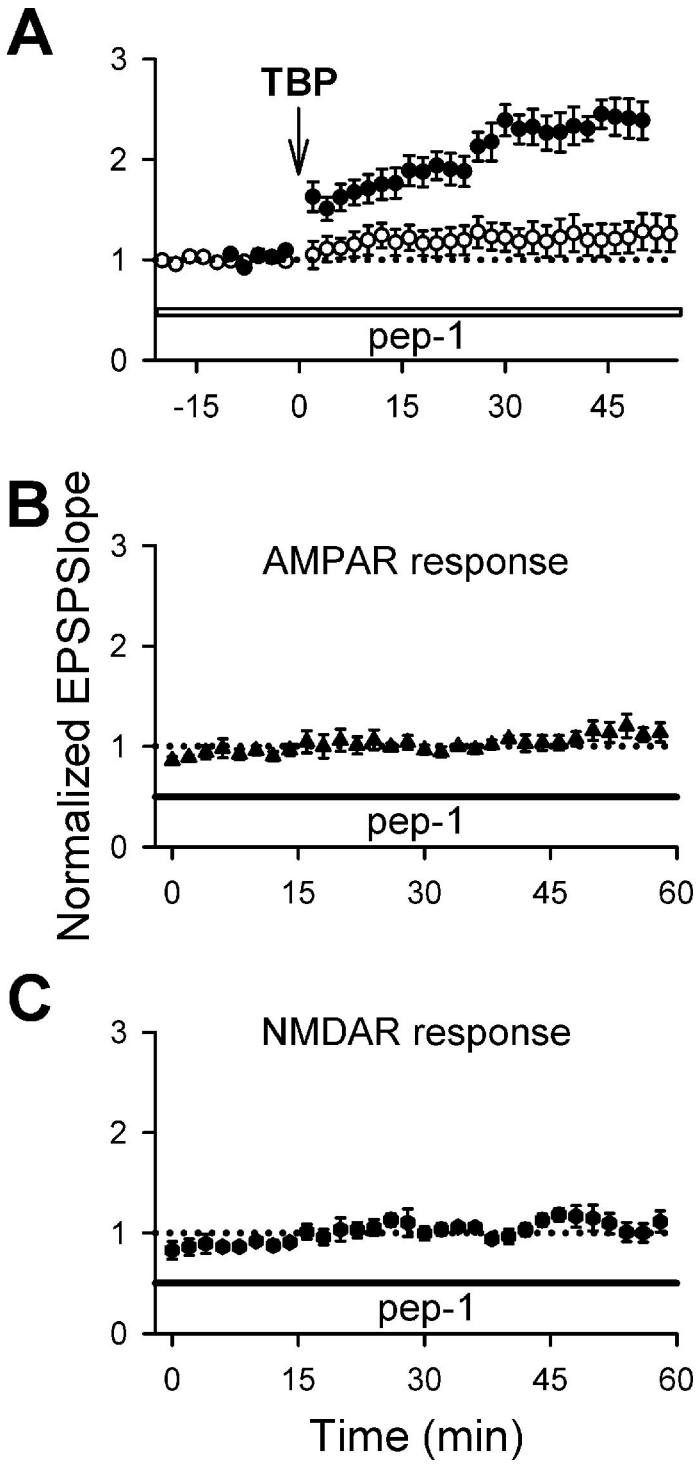

Fig. S5. Postsynaptic loading of a peptide mimicking the GluR1 C-terminal blocks LTP. (*A*) Postsynaptic loading of the pep-1 peptide abolished LTP (124 ± 16% at 45–50 min after TBP, $n = 14$, open symbols; $P < 0.01$, as compared with control LTP, filled symbols). (*B*) Postsynaptic loading of pep-1 did not affect AMPAR EPSPs at naïve synapses ($n = 6$). (*C*). Postsynaptic loading of pep-1 did not affect NMDAR EPSPs at naïve synapses ($n = 6$).

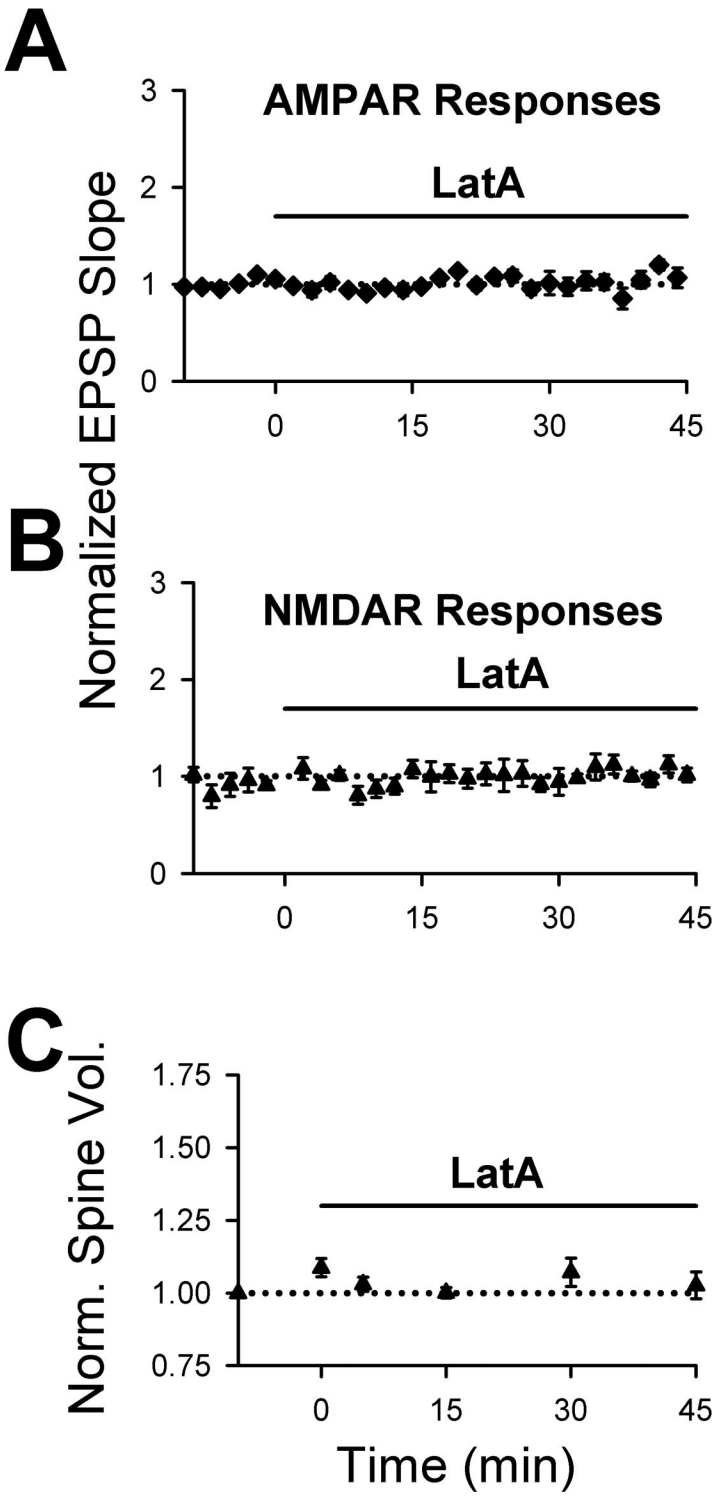

Fig. S6. Bath perfusion of latA does not affect synaptic transmission or spine size. (*A*) Bath perfusion of latA did not affect basal synaptic transmission (102 ± 6%; $n = 7$). (*B*) LatA did not alter NMDA receptor-mediated EPSPs (100 ± 9%; $n = 5$). (*C*) LatA had no effect on spine size at native synapses ($n = 46$ spines/4 cells).

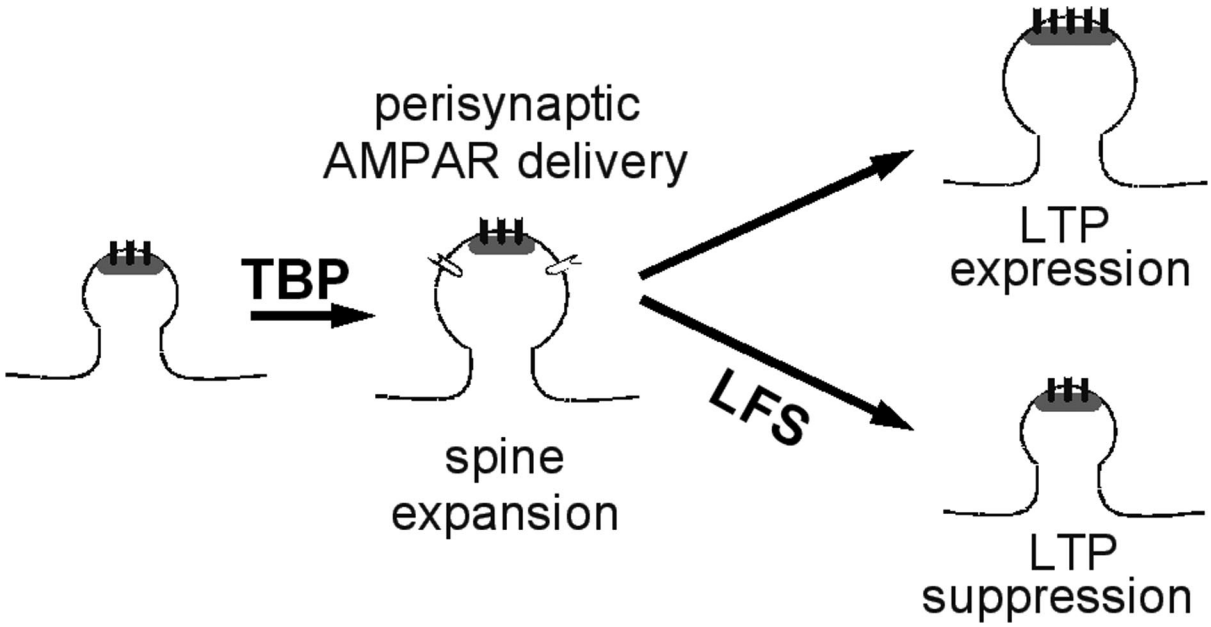

Fig. S7. A proposed model. A model is shown in which LTP expression occurs in two steps, delivery of AMPARs to the perisynaptic region, followed by translocation into the synapse. Suppression of LTP by LFS takes place by removal of perisynaptic AMPARs before translocation. Spine expansion occurs simultaneously with the delivery of perisynaptic AMPARs but is not required for this first step; it remains unclear whether spine expansion is somehow involved in the eventual expression of LTP.